All-sky radiative transfer calculations for IASI and IASI-NG: The σ_IASI-as code

G. Liuzzi, M. G. Blasi, G. Masiello, C. Serio, and S. Venafra

Citation: AIP Conference Proceedings **1810**, 040004 (2017); doi: 10.1063/1.4975506
View online: http://dx.doi.org/10.1063/1.4975506
View Table of Contents: http://aip.scitation.org/toc/apc/1810/1
Published by the American Institute of Physics

All-Sky Radiative Transfer Calculations For IASI And IASI-NG: The σ-IASI-as Code

G. Liuzzi[1, a), b)], M. G. Blasi[1, c)], G. Masiello[1, d)], C. Serio[1, e)] and S. Venafra[1, f)]

[1] *Scuola di Ingegneria, Università della Basilicata, via Ateneo Lucano, 10, 85100 Potenza, Italy.*

a)Corresponding author: giuliano.liuzzi@unibas.it
b)URL: http://www2.unibas.it/gmasiello/assite/as/home.html
c)maria.blasi@unibas.it
d)guido.masiello@unibas.it
e)carmine.serio@unibas.it
f)sara.venafra@unibas.it

Abstract. In the context of the development by EUMETSAT of a new generation of meteorological satellites, we have built the new σ-IASI-as (where "as" stands for "all sky") radiative transfer code. Unlike its predecessor σ-IASI, the code is able to calculate both clear and cloudy sky radiances, as well as their Jacobians with respect to any desired geophysical parameter. In addition, σ-IASI-as can perform calculations to simulate the extinction effect of the most common types of atmospheric aerosols and of clouds via ab-initio Mie calculations. We briefly describe the analytical scheme on which the model is based, and have a glance to its potentialities illustrating some sample calculations. Overall, the new model is a complete and fast radiative transfer tool for IASI, and already available for IASI-NG and MTG-IRS.

INTRODUCTION

In order to give continuity in the service offered by the Infrared Atmospheric Sounder Interferometer (IASI, [1]), EUMETSAT has scheduled the workability of a new generation of instruments, named IASI-NG (IASI New Generation). IASI-NG is a key element of the MetOp-SG, a series of European meteorological polar-orbit satellites. IASI-NG is intended also to offer enhanced technical performances with respect to IASI, as far as spectral resolution and signal-to-noise ratio are concerned. The new generation of IASI, together with the Third Generation of Meteosat geostationary platforms (MTG) scheduled by EUMETSAT in the next years, and the scientific perspectives of these new instruments, make of absolute importance the availability of a complete radiative transfer model to simulate the radiance as it is observed by IASI-NG, MTG-IRS (InfraRed Sounder), also adaptable to any other similar instrument, for scientific and operational purposes.
This paper describes the new radiative transfer code σ-IASI-as, which has been conceived to be an update of the σ-IASI code [2], as far as the possibility to simulate all-sky conditions is concerned. Nevertheless, this new code holds intact its basic mathematical framework for the calculation of radiance and its derivatives (namely, Jacobians), and its feasibility with respect to the possibility to work with any instrumental response function. We will show some sample calculations for different sky conditions.

RADIATIVE TRANSFER SCHEME

Most of the radiative transfer model is described in detail in [2,3]. Here we limit ourselves to recall only the main elements of the way in which the radiative transfer is implemented. The expression of the radiance that is handled by the σ-IASI-as model works within the hypothesis that the instrument observes an homogeneous field of view (FOV),

Radiation Processes in the Atmosphere and Ocean (IRS2016)
AIP Conf. Proc. 1810, 040004-1–040004-4; doi: 10.1063/1.4975506
Published by AIP Publishing. 978-0-7354-1478-5/$30.00

without weird effects such as shadows or inhomogeneous cloud borders. Geophysical parameters vary only along the observation direction. Moreover, the model is optimized to work from the far to the near infrared (3-100 μm).
In these hypotheses, if α denotes the cloudy portion of the FOV, the observed radiance will be written as the sum of two contributions, one for clear sky and one for the overcast part of the FOV [4]:

$$R(\sigma) = (1-\alpha)R_c(\sigma) + \alpha R_N(\sigma) \tag{1}$$

The two terms of radiance are computed by the code using a pseudo-monochromatic approach, which is far faster than line-by-line approach. The atmosphere is divided into 60 layers (covering the pressure interval 1013-0.005 mbar), whose pressure boundaries are fixed, and considered to be homogeneous in temperature and composition. Hence, the number of layers used to describe the atmospheric structure is dependent on the surface pressure, namely on the air mass above the observed target. With this structure, the two radiance contributions are computed by the code as follows (the subscript is referred to the first term, but the second one is formally analogous):

$$R_c = \varepsilon_g B(T_g)\tau_{0,c} + \sum_{j=1}^{N_L} B(T_j)\,(\tau_{c,j} - \tau_{c,j-1}) + (\varepsilon_g - 1)\sum_{j=1}^{N_L} B(T_j)\,(\tau_{c,j}^{-1} - \tau_{c,j-1}^{-1}) + \frac{1-\varepsilon_g}{\pi}\tau_c'\mu_s I_s \tag{2}$$

where, respectively: the first term represents the radiance directly emitted by the surface, with a skin temperature T_g, an emissivity $\varepsilon_g(\sigma)$, and attenuated by the atmospheric column above surface, whose total transmittance is $\tau_0(\sigma)$; the second term represents the upwelling radiance, namely the radiance emitted directly from the atmosphere along the slant path in the viewing direction, integrated along the whole path; the third term expresses the down welling radiance, which is the radiance contribution emitted from the atmosphere towards surface, that is back-reflected from it and then reaches the observer; finally, the last term represents the solar radiance I_s/π reflected back from surface and then reaching the observer, with τ' the two-way transmittance along the path Sun-surface-observer, and μ_s the cosine of the solar zenith angle. The transmittances that appear in the sums in Equation (2) are the cumulative transmittances, namely computed from the top of the atmosphere to the bottom of the j-th layer. The model assumes that the clear sky transmittances are affected by the attenuation due to gases and aerosols, while the cloudy sky ones are determined by gases, aerosols and clouds optical depths. Both gases and aerosols/clouds are treated in the context of a "pure absorption" approach, hence the optical depth due to the i-th absorber (whatever it is) in the j-th layer is expressed as

$$\chi_{i,j}(\sigma) = q_{i,j}k_{i,j}(\sigma)\Delta h_j \tag{3}$$

where $q_{i,j}$ is the concentration of the i-th species in the j-th layer, $k_{i,j}$ (σ) is the absorption coefficient for that species at wave number σ, and Δh_j denotes the path length, along the observation direction, from the bottom of the j-th layer to its top.The absorption coefficient is computed according to two different approaches, one for gases and another for clouds and aerosols.
For gases, the code embodies a wide look-up table where, for each layer, and for a set of atmospheric species and wave numbers, optical depths are pre-computed and stored. Gases optical depths should vary with air pressure and temperature: on the one hand, pressure is fixed by the atmospheric layering; on the other hand, the dependence on temperature is parameterized: optical depths are generated using the version 12.2 of LBLRTM [5], using as input parameters the reference U.S. Standard Atmosphere [6]. Optical depths are then re-calculated using the same temperature profile translated by eight evenly spaced temperature values going from -40 K to + 40 K. This interval is large enough to account for the usual temperature variations that characterize Earth's atmosphere. Once optical depths are calculated, for each individual species (except for water vapour), layer and wave number, the behaviour of the optical depth is parameterized by a second order polynomial in the temperature. Water vapour optical depth, instead, is modelled by a slightly different parameterization, in order to take into account the effects depending on gas concentration, such as self-broadening, we use a further coefficient which multiplies the water vapour concentration. The look-up table used by σ-IASI-as embodies parameterizations for water vapour (H_2O), carbon dioxide (CO_2), ozone (O_3), nitrous oxide (N_2O), carbon monoxide (CO), methane (CH_4), sulphur dioxide (SO_2), nitric acid (HNO_3), ammonia (NH_3), carbonyl sulphide (OCS) and CF_4 [7]. The other gases (among them ChloroFluoroCarbons (CFCs), O_2 and N_2) are included in an unique parameterization, which we refer to as mixed gases. Calculations are performed at a resolution of 10^{-2} cm^{-1}. Apart from the contribution to optical depths due to absorption lines, the code computes also the continuum absorption, which is typical of O_2, N_2, and water vapour, using the parametric model MT-CKD, v2.5.2 [8].

For aerosols and clouds, the scheme exploits directly the Mie theory [9], which solves the set of Maxwell's equations describing the scattering of an electromagnetic plane wave by an homogeneous sphere. In addition, the model implements the scheme described in [10] to reckon the effective aerosol/cloud optical depth, which is modelled as the sum of two terms, being the first one the absorption efficiency β_{abs} as calculated by the Mie code, and the second a term which parameterizes the multiple scattering effects through the single scattering albedo ω and the scattering phase function β, which is assumed to have the form of the Henyey-Greenstein phase function, and is further expressed as a third order polynomial of the asymmetry factor g, with fixed coefficients:

$$k(\sigma) = \beta_{abs}(\sigma) + \beta_{ext}(\sigma)b(\sigma)\omega(\sigma) \tag{4}$$

All the quantities involved in the aerosol/cloud extinction calculations depend on the microphysical properties of particles, namely their dimensional distribution and their complex refractive indices. The σ-IASI-as works with a superposition of an arbitrary number of log-normal modes for the most common atmospheric aerosol types. In order to limit the computational load due to reckon the aerosols optical depth, the code is structured in such a way to minimize the number of calls to the Mie routines. Since absorption features due to aerosols and cloud particles have a very smooth spectral behaviour, calculations are performed on a wave number grid with a sampling of 15 cm^{-1}, which is fine enough to correctly reproduce the absorption features of all the atmospheric aerosols. Results are then interpolated on the wave number grid used to compute gases optical depths. The aerosols handled by the code are summarized in Table 1.

TABLE 1. List of the aerosols included in the σ-IASI-as model. (a) sea salt refractive indices are tabulated for eight different values of relative humidity, ranging from 0% to 99%. (b) H_2SO_4 droplets are tabulated for two temperature values: 215 K and 300 K. (c) since these materials are birefringent, for each of them there are two sets of refractive indices, one for the ordinary light ray, and the other for the extraordinary one. These sets are largely convenient in case the σ-IASI-as model is used to simulate polarized radiances.

Aerosol types		
Water droplets	*Ice crystals*	Hydrophilic aerosol
NaCl	Sea salt [(a)]	NH_3 droplets
Carbonaceous aerosol	Volcanic dust	Meteoric dust
H_2SO_4 droplets [(b)]	Volcanic ash	Saharan dust
Quartz [(c)]	Hematite [(c)]	Desert sand [(c)]
Ammonium sulphate	Burning vegetation ash	Flame soot

CODE PERFORMANCES AND SAMPLE CALCULATIONS

The fully analytical parameterization by which the code computes gases optical depths, and the semi-analytical way in which aerosols and clouds are treated, are useful to make the code faster, and also to compute analytical radiance Jacobians of the main geophysical parameters. As already stated, the code treats separately 12 gaseous species, for which it can be computed the Jacobian with respect to concentration. In addition, the code can compute the Jacobians with respect to atmospheric temperature profile, and surface temperature and emissivity (details in [2]). Moreover, one of the most relevant features of σ-IASI-as is its capability to deal with different surface types, hence different reflection geometries from surface, both Lambertian (e.g. on most of land surfaces) and specular (e.g. on the sea surface), without any degradation of code performances.

Code computational performances are in line to most of the fast, parametric radiative transfer models used in the context of Numerical Weather Predictions (NWP) and similar applications: the model can compute the radiance of 20 spectral channels in 0.004 s on modern CPUs, and it takes about 1.5 s to compute a single IASI spectrum (8461 channels), and 0.1 s more to add aerosol/cloud extinction.

To have a glance to the code capabilities, we show here a comparison between radiances computed by the model using as input the atmospheric profiles and surface parameters provided by the European Centre for Medium range Weather Forecasts (ECMWF) and the radiances as observed by the Spinning Enhanced Visible and InfraRed Imager (SEVIRI) on board the Meteosat Second Generation (MSG) platform. Observations and ECMWF data correspond both to 1 April 2013; we consider the whole Mediterranean basin. Figure 1 provides a quick comparison between simulated and observed radiances, for two different hours and spectral channels to better highlight the capability of the code to reproduce the observed radiance both in presence and absence of solar radiation. We can see that no

significant differences occur, neither in the channel at 3.9 µm, which is centred in a spectral atmospheric window, nor in that at 7.3 µm, which instead is also sensitive to the structure of upper troposphere and stratosphere. Other minor differences are due to some well-known biases in ECMWF analyses [11], because we do not perform any residuals' minimization [12,13], but simply we compare simulations and observations.

Figure 2, instead, shows an example of spectra, computed at IASI-NG resolution, with and without the extinction due to an ice cloud located in the upper troposphere (whose profile in terms of particles concentration is reported on the right). The average radius of ice particles chosen for the simulation is 12 µm. We can see how the code correctly reproduces the typical spectral signature of the water ice around 800 cm^{-1}.

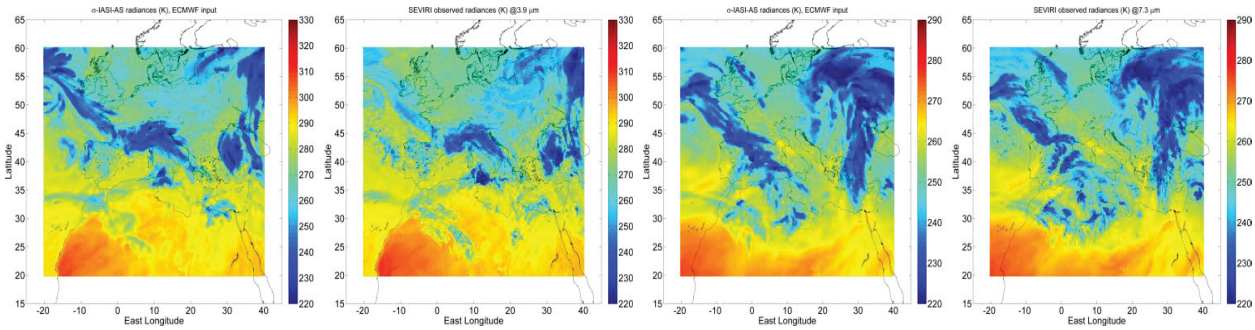

FIGURE 1. From the left to the right. First and second panels: simulated and observed radiances in the SEVIRI channel centred at 3.9 µm at 18 UTC of 1 April 2013. Differences are visible only in cloudy areas, where solar reflected radiation can be significant. Third and fourth panel: Same as the others, but for the SEVIRI channel at 7.3 µm at 0 UTC.

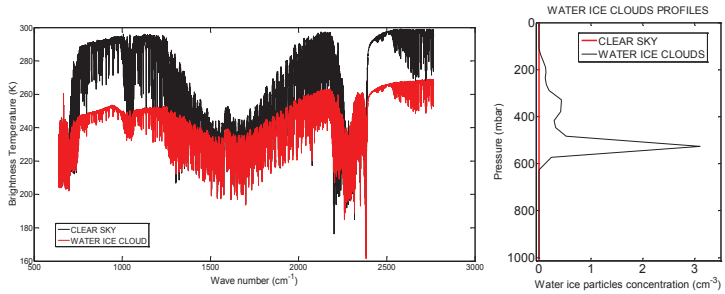

FIGURE 2. Left panel: IASI-NG spectra computed in absence (black) and presence (red) of an ice cloud, whose particle concentration profile is reported in the right panel.

REFERENCES

1. F. Hilton et al, Bulletin of the American Meteorological Society, **93**(3), 347-370, (2012).
2. U. Amato, G. Masiello, C. Serio, and M. Viggiano, Environmental Modelling & Software, **17**(7), 651-667, (2002).
3. G. Liuzzi et al, Journal of Physics, Conference Series, **633**(1), 012059, (2015).
4. M. T. Chanine, Journal of the Atmospheric Sciences, **31**, 233-243, (1974).
5. S. A. Clough et al, J. Quant. Spectrosc. Rad. Transfer, **91**, 233-244, (2005).
6. G. P. Anderson et al, Geophysics Laboratory, Hanscom Air Force Base, USA, (1986).
7. G. Liuzzi et al, J. Quant. Spectrosc. Rad. Transfer, **182**, 128-157, (2016).
8. E. J. Mlawer et al, Phil. Trans. R. Soc. A, **370**, 1-37, (2013).
9. C. F. Bohren and D. R. Huffmann, Wiley-Interscience, New York, NY, USA, (2000).
10. M.-D. Chou, K.-T. Lee, S.-C. Tsay, and Q. Fu, Journal of Climate, **12** (1), 159-169, (1999).
11. G. Masiello, M. Matricardi, and C. Serio, Atmos. Chem. Phys., **11** (3), 1009-1021, (2011).
12. G. Grieco, G. Masiello, and C. Serio, Remote Sensing, **2**(10), 2323-2346, (2010).
13. U. Amato, A. Antoniadis, I. De Feis, G. Masiello, M. Matricardi, and C. Serio, Atmos. Chem. Phys., **9**(14), 5321-5330, (2009).